A Thin Dielectric Approximation for Calculation of Electromagnetic Scattering from 3-D Homogeneous Chiral Bodies

X. Deng[1], Y. Tian[1], J. Wang[2] , C. Gu[3], and Y. Zhou [3]

[1] Department of Electronic Information, Jiangsu University of Science and Technology, Zhenjiang 212003, China
dengxiaoqiao_521@163.com, yubo.tian@163.com

[2] State Key Laboratory of Millimeter Waves, School of Information Science and Engineering, Southeast University, Nanjing 210016, China
wangjian.seu@hotmail.com

[3] College of Electronic and Information Engineering, Nanjing University of Aeronautics and Astronautics, Nanjing 210016, China
gucq0138@sina.com, iamrealzyg@yahoo.com.cn

Abstract ─The full current thin dielectric sheet (TDS) approximation is considered for the problem of electromagnetic (EM) scattering by a three-dimensional (3-D) homogeneous thin chiral dielectric sheet. This approximation leads to surface integral equations (SIE) instead of the traditional volume integral equations (VIE). The surface of the thin dielectric region is modeled by triangle cells. Consequently, the number of unknowns is reduced by only surface meshes being utilized to discretize the dielectric geometry. Modified Rao-Wilson-Glisson (RWG) and pulse functions simultaneously for basis and testing functions are employed to approximate the tangential and normal currents in the dielectric layer. Then these SIEs are solved numerically using the conventional method of moments (MoM). The results by this approach show agreement with other methods while it greatly reduces the number of unknowns.

Keywords ─ Electromagnetic (EM) scattering, method of moments (MoM), pulse basis functions, Rao-Wilson-Glisson (RWG) basis functions, surface integral equations (SIE), thin dielectric sheet (TDS), and volume integral equations (VIE).

I. INTRODUCTION

Over recent years, many works have been contributed in an effort to develop efficient numerical techniques to solve the electromagnetic (EM) problems related to three-dimensional (3-D) chiral materials [1-4]. In [1], the finite-difference time-domain (FDTD) method was extended for chiral bodies. In [2], the transition matrix (T-matrix) method has been modified for chiral scatterer. However, each of these methods has certain limitations. In solving problems involving dispersive materials, time domain methods rely on the Z-transform of analytical expressions that describe dispersion properties of a material. The convergence problem restricts T-matrix's application. Extensive literatures in this area show a continuous interest in the method of moments (MoM) technique for solving EM problems related to chiral bodies [3, 4]. The MoM based on surface integral equation (SIE) method has been applied to deal with chiral problems [3]. For complex bodies consisting of inhomogeneous chiral media, the generalizing volume integral equation (VIE) method involving MoM has been extended to solve the EM scattering [4]. As we all well know, volumetric formulations have been widely used in calculating the electromagnetic scattering from arbitrarily shaped, inhomogeneous, dielectric bodies, however, it is also well known that

Submitted On: Sept. 4, 2012
Accepted On: Jan. 19, 2014

burdened with the discretization of the object and the surrounding space, the number of unknowns of VIE rapidly grows with the size of the object, this results in larger memory requirement and longer solution time in solving the corresponding matrix equation, it limits the application of the simulation in the case of large and open radiation problems. The VIE is suitable for inhomogeneous dielectric structures. However, both VIE and general SIE only work well for relatively thick dielectric materials. They tend to suffer from unfavorable convergence problems when the dielectric is thin, especially less than one tenth of a wavelength in dielectric.

By the way, more and more nonmetallic structures have replaced metallic ones to reduce the weight or the radar cross section (RCS), especially in the construction of radome, so that an investigation of a thin dielectric layer is very important. For a very thin dielectric, a method called impedance boundary condition (IBC) algorithm has been extensively applied to analyze the thin and lossy dielectric coating problems [5]. In this way, the geometry is modeled by surface meshes for the SIE instead of volume meshes for the VIE. The unknown quantity is then greatly reduced, and the resultant SIE based on the IBC is then solved by MoM using the popular RWG basis. The algorithm can greatly facilitate the solving of EM scattering problems involving thin dielectric. Although the IBC method has a high computational efficiency, there still have some constraints of the algorithm because of its plane wave approximation. Another method for solving thin dielectric sheet problems is the thin dielectric sheet (TDS) approximation [6]. In this approximation, the algorithm adopts the assumption that the induced volume current remains constant and very small in the normal direction because the thickness of the dielectric sheet is relatively small compared to the wavelength, then only the tangential field component is considered, that is the contribution from the normal polarization current was ignored. In order to improve the accuracy of the equivalent model of TDS, a modified TDS approximation referred as the full current TDS approximation [7, 8] takes both tangential and normal currents into account, and the normal currents are described by the additional vector pulse basis functions in the algorithm. It can handle the EM scattering problem of TDS more efficiently. The full current TDS approximation is then extended to deal with the scattering problem for multilayer dielectric sheets and coating objects [9, 10].

As a generalization work of the previous methods, the main contribution of this paper therefore is that the full current TDS approximation strategy is extended and applied to the scattering problems for thin chiral dielectric sheet. The rest of the paper is organized as follows. Section 2 gives a concise introduction to the full current TDS formulations derived from VIE equations to describe electromagnetic scattering involving thin chiral dielectric sheet. In section 3, The MoM solution procedure and matrix evaluation are described. Numerical examples are demonstrated and discussed in section 4. Last but not least, some concluding remarks are given in section 5.

II. FORMULATION

A. TDS surface integral formulation

Let us consider a thin homogeneous bi-isotropic sheet, as illustrated in Fig. 1. The geometry is assumed to be illuminated by a plane wave incident fields $\mathbf{E}^{inc}, \mathbf{H}^{inc}$. The expressions of electric and magnetic fields inside the bi-isotropic region are relatively complex due to the introduction of bi-isotropic constitutive relations, namely,

$$\mathbf{D} = \varepsilon \mathbf{E} + \xi \mathbf{H} \tag{1}$$

$$\mathbf{B} = \mu \mathbf{H} + \zeta \mathbf{E}, \tag{2}$$

where ε and μ are the permittivity and permeability, respectively, ξ and ζ are bi-isotropic parameters. $\mathbf{E}$, $\mathbf{H}$, $\mathbf{D}$, and $\mathbf{B}$ are the complex-valued phasors of the electric field, magnetic field, displacement vector, and magnetic induction intensity, respectively. And the $\mathbf{D}$ and $\mathbf{B}$ can be also written as,

$$\mathbf{D} = \varepsilon \mathbf{E} + (\chi_r - i\kappa_r)\sqrt{\varepsilon\mu}\mathbf{H} \tag{3}$$

$$\mathbf{B} = \mu \mathbf{H} + (\chi_r + i\kappa_r)\sqrt{\varepsilon\mu}\mathbf{E}, \tag{4}$$

where κ_r and χ_r are chirality parameter and tellegen parameter, respectively. A bi-isotropic medium with $\chi_r = 0$ and $\kappa_r = 0$ is an ordinary magneto-dielectic medium, the one with $\chi_r = 0$ and $\kappa_r \neq 0$ then is called chiral medium, while the one with $\chi_r \neq 0$ and $\kappa_r = 0$ is named Tellegen medium.

In the paper, we only study the chiral problem as a special case. However, the method is applicable to any thin bi-isotropic media situation.

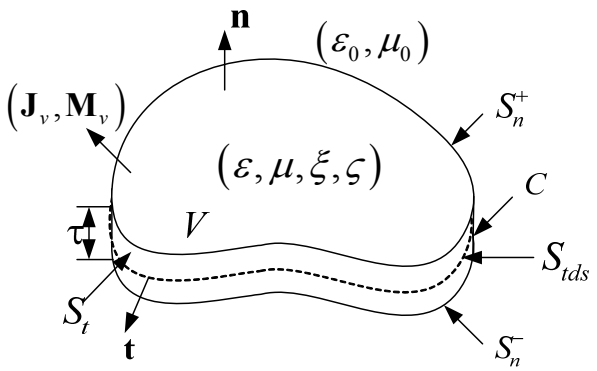

Fig. 1. Configuration of a thin chiral sheet.

Then $\mathbf{E}$, $\mathbf{H}$ can be expressed as,

$$\mathbf{E} = \alpha_1 \mathbf{D} + \alpha_2 \mathbf{B} \tag{5}$$

$$\mathbf{H} = \alpha_3 \mathbf{D} + \alpha_4 \mathbf{B}, \tag{6}$$

where the parameters $\alpha_i (i = 1,2,3,4)$ are given by equations (26) to (29) in the appendix.

The polarization volume electric/magnetic current density in the chiral dielectric are defined by,

$$\mathbf{J}_v = i\omega\beta_1 \mathbf{D} + i\omega\beta_2 \mathbf{B} \tag{7}$$

$$\mathbf{M}_v = i\omega\beta_3 \mathbf{D} + i\omega\beta_4 \mathbf{B}, \tag{8}$$

where the parameters $\beta_i (i = 1,2,3,4)$ are given by equations (30) to (33) in the appendix.

Inside the thin dielectric medium, the incident electric field, scattered electric field, and total electric field satisfy,

$$\mathbf{E}^{inc}(\mathbf{r}) = \mathbf{E} - \mathbf{E}_{die}^{scat}(\mathbf{r}), \quad \mathbf{r} \in V \tag{9}$$

where $\mathbf{E}_{die}^{scat}$ stands for the scattered electric field from the TDS, $\mathbf{r}$ denotes the field point. Similarly, by electric-magnetic duality in Maxwell theory, the relationships among the incident magnetic field, scattered magnetic field, and total magnetic field in the thin sheet can be expressed as,

$$\mathbf{H}^{inc}(\mathbf{r}) = \mathbf{H} - \mathbf{H}_{die}^{scat}(\mathbf{r}), \quad \mathbf{r} \in V \tag{10}$$

where $\mathbf{H}_{die}^{scat}$ stands for the scattered magnetic field from the TDS. Scattering electric and magnetic fields from the dielectric region are written as,

$$\mathbf{E}_{die}^{scat}(\mathbf{r}) = -i\omega\mu_0 \int_v G(\mathbf{r},\mathbf{r}')\mathbf{J}_v(\mathbf{r}')dV' + \frac{\nabla}{i\omega\varepsilon_0}\int_v G(\mathbf{r},\mathbf{r}')\left(\nabla' \cdot \mathbf{J}_v(\mathbf{r}')\right)dV' - \nabla \times \int_v G(\mathbf{r},\mathbf{r}')\mathbf{M}_v(\mathbf{r}')dV' \tag{11}$$

$$\mathbf{H}_{die}^{scat}(\mathbf{r}) = -i\omega\varepsilon_0 \int_v G(\mathbf{r},\mathbf{r}')\mathbf{M}_v(\mathbf{r}')dV' + \frac{\nabla}{i\omega\mu_0}\int_v G(\mathbf{r},\mathbf{r}')\left(\nabla' \cdot \mathbf{M}_v(\mathbf{r}')\right)dV' - \nabla \times \int_v G(\mathbf{r},\mathbf{r}')\mathbf{J}_v(\mathbf{r}')dV' \tag{12}$$

where $G(\mathbf{r},\mathbf{r}')$ is the scalar Green's function in free space which is defined by $G(\mathbf{r},\mathbf{r}') = \frac{e^{ik_0|\mathbf{r}-\mathbf{r}'|}}{4\pi|\mathbf{r}-\mathbf{r}'|}$. The thickness of dielectric layer is quite limited compared to the wavelength, so the fields vary very little with respect to the normal direction. Volume integral can be replaced by the surface integral at the middle section, as,

$$\int_v dV' \approx \tau \int_{S_{tds}} dS'. \tag{13}$$

Thus, the volume integrals degenerate to surface integrals and the number of unknowns is evidently reduced because only surface meshes are utilized to discretize the geometry. In addition, to transform the volume integrals in equations (11) and (12) to surface integrals, it is necessary to decompose the $\mathbf{D}$ and $\mathbf{B}$ into tangential and normal components within the TDS, that is,

$$\mathbf{D} = \mathbf{D}_t + \mathbf{D}_n \tag{14}$$

$$\mathbf{B} = \mathbf{B}_t + \mathbf{B}_n. \tag{15}$$

According to [7],

$$\nabla \cdot (\beta_i \mathbf{D}) = \nabla\beta_i \cdot \mathbf{D} + \beta_i \nabla \cdot \mathbf{D} = \nabla\beta_i \cdot \mathbf{D}, \quad (i = 1,2) \tag{16}$$

and take equations (7), (8), (13), and (16) into equations (11) and (12), the integrals in equations (11) and (12) then can be approximated as,

$$\begin{aligned}\mathbf{E}_{die}^{scat}(\mathbf{r}) = {} & \omega^2\mu_0\tau\int_{S_{tds}} G(\beta_1\mathbf{D})dS' + \frac{\nabla}{\varepsilon_0}\oint_{S_t+S_n^+ +S_n^-} G\Delta\beta_1\mathbf{n}' \cdot \mathbf{D}dS' \\ & + \omega^2\mu_0\tau\int_{S_{tds}} G(\beta_2\mathbf{B})dS' + \frac{\nabla}{\varepsilon_0}\oint_{S_t+S_n^+ +S_n^-} G\Delta\beta_2\mathbf{n}' \cdot \mathbf{B}dS' \\ & - i\omega\tau\beta_3\int_{S_{tds}} \nabla G \times \mathbf{D}dS' - i\omega\tau\beta_4\int_{S_{tds}} \nabla G \times \mathbf{B}dS'\end{aligned} \tag{17}$$

$$\mathbf{H}_{die}^{scat}(\mathbf{r}) = \omega^2\varepsilon_0\tau\int_{S_{tds}} G(\beta_3\mathbf{D})dS' + \frac{\nabla}{\mu_0}\oint_{S_t+S_n^+ +S_n^-} G\Delta\beta_3\mathbf{n}'\cdot\mathbf{D}dS' + \omega^2\varepsilon_0\tau\int_{S_{tds}} G(\beta_4\mathbf{B})dS' + \frac{\nabla}{\mu_0}\oint_{S_t+S_n^+ +S_n^-} G\Delta\beta_4\mathbf{n}'\cdot\mathbf{B}dS' - i\omega\tau\beta_1\int_{S_{tds}}\nabla G\times\mathbf{D}dS' - i\omega\tau\beta_2\int_{S_{tds}}\nabla G\times\mathbf{B}dS' \quad (18)$$

where S_n^+, S_n^-, S_t, S_{tds} denote top, bottom, side, and middle surfaces, respectively, and $\mathbf{n}'$ is the unit normal vector directing out of the TDS at the interfaces. Take equations (14) and (15) into equations (17) and (18), the formulas (34) and (35) for $\mathbf{E}_{die}^{scat}$ and $\mathbf{H}_{die}^{scat}$ can be further obtained. Then the TDS SIEs are obtained by taking equations (34) and (35) into equations (9) and (10).

B. MoM solution

Because the electric flux in equation (14) is decomposed into normal and tangential parts, it can be specified by two sets of basis functions numerically. It is the same to magnetic intensity in equation (15). As a result, to solve the TDS SIEs by the MoM, four sets of basis functions are employed. For TDS, the modified RWG basis [7] is used for the tangential current since charge is enforced to exist at the edges between air-dielectric interfaces, and the pulse basis [7-8] is used for the normal current. The difference between the modified RWG basis and the conventional RWG basis [11] is that the former defines half basis functions at the edges. The electric flux and magnetic intensity are approximated by four sets of basis functions as follows,

$$\mathbf{B}_t \approx \sum_{d=1}^{N_d} B_d\mathbf{f}_d(\mathbf{r}) \quad (19)$$

$$\mathbf{B}_n^+ \approx \sum_{n=1}^{N} B_n\mathbf{P}_n(\mathbf{r}), \quad (20)$$

$$\mathbf{D}_t \approx \sum_{d=1}^{N_d} D_d\mathbf{f}_d(\mathbf{r}), \quad (21)$$

$$\mathbf{D}_n^+ \approx \sum_{n=1}^{N} D_n\mathbf{P}_n(\mathbf{r}), \quad (22)$$

where N_d is the number of total edges (including shared and boundary edges) and N is the total number of triangles T_n of the TDS. $\mathbf{f}_d(\mathbf{r})$ is the modified RWG basis defined as,

$$\mathbf{f}_d(\mathbf{r}) = \begin{cases} \dfrac{l_d}{2A_d^{\pm}}\boldsymbol{\rho}_d^{\pm} & \mathbf{r}\in T_d^{\pm} \\ 0 & otherwise \end{cases} \quad (23)$$

where l_d is the length of the edge and $A_d^{\pm}$ is the area of the corresponding triangle $T_d^{\pm}$. It should be noted that for half basis, only A_d^+ is defined at the boundary edges of an open surface. $\mathbf{P}_n(\mathbf{r})$ is the vector pulse basis of triangles, defined as,

$$\mathbf{P}_n(\mathbf{r}) = \begin{cases} \mathbf{n}_n & \mathbf{r}\in T_n \\ 0 & \mathbf{r}\notin T_n \end{cases} \quad (24)$$

where $\mathbf{n}_n$ is the unit normal vector of the triangle T_n.

To convert the TDS SIEs into matrix equations, by Galerkin's testing procedure, we test the TDS SIEs with the modified RWG basis and pulse basis. The matrix equation $[Z][I]=[V]$ can be written as,

$$\begin{bmatrix} Z_{TT}^{DD} & Z_{TN}^{DD} & Z_{TT}^{DB} & Z_{TN}^{DB} \\ Z_{NT}^{DD} & Z_{NN}^{DD} & Z_{NT}^{DB} & Z_{NN}^{DB} \\ Z_{TT}^{BD} & Z_{TN}^{BD} & Z_{TT}^{BB} & Z_{TN}^{BB} \\ Z_{NT}^{BD} & Z_{NN}^{BD} & Z_{NT}^{BB} & Z_{NN}^{BB} \end{bmatrix}\begin{bmatrix} D_d \\ D_n \\ B_d \\ B_n \end{bmatrix} = \begin{bmatrix} V_t^E \\ V_n^E \\ V_t^H \\ V_n^H \end{bmatrix} \quad (25)$$

where the subscript *TT* denotes the interaction between tangential current, *TN* and *NT* denotes the interaction between tangential and normal current, *NN* denotes the interaction between normal current. The superscript alphabet *D* and *B* involves electric current and magnetic current, respectively. V_t^E and V_t^H denote the excitation from incident tangential electric and magnetic fields, and V_n^E and V_n^H denote the excitation from incident normal electric and magnetic fields. B_d and D_d are $N_d\times 1$ unknown matrices, and D_n and B_n are $N\times 1$ unknown matrices. The elements of $[Z]$ are given in the appendix.

III. NUMERICAL RESULTS

In this section, three examples are investigated. Only chiral problems are considered as a special case, so $\chi_r = 0$ in the following examples. The first example is a dielectric sphere shell under the illumination of a plane wave incident from the direction where $(\theta,\varphi)=(0^\circ,0^\circ)$ at 0.2 GHz. The sphere is with inner radius 1.0 m, outer radius 1.05m, and $\varepsilon_r = 2.6$, $\mu_r = 1$, $\kappa_r = 0$. It is modeled

by 1866 triangles. Figure 2 (a) and (b) show the total RCS at $\varphi = 0^{\circ}$ and $\varphi = 90^{\circ}$. The circle lines by our proposed TDS SIE agree well with the solid lines by the Mie series.

In the second example, we consider a thin chiral plate as an example. In order to demonstrate the validity and advantages of our method, the results calculated by VIE are also given for comparison. The dimension of the chiral plate is $1m \times 0.5m \times 0.05m$ (in x, y, and z dimensions, respectively), and the constitutive parameters are $\varepsilon_r = 2.6$, $\mu_r = 1$, and $\kappa_r = 0$, 0.1, 0.3, 0.5, 0.7. The structure is illuminated by a plane wave incident from the direction where $(\theta, \varphi) = (180^{\circ}, 0^{\circ})$. It is modeled by 400 triangles for the TDS SIE and 1369 tetrahedrons for VIE. Figure 3 shows the normalized co-polarized and cross-polarized bistatic RCS ($\sigma_{\theta\theta}/\lambda_0^2$ and $\sigma_{\phi\theta}/\lambda_0^2$) for scattering angle $\varphi = 0^{\circ}$ calculated by our code and VIE. In order to show more clearly, the curves calculated by VIE are plotted only when $\kappa_r = 0.5$. From Fig. 3, we can conclude that they are in good agreements. Small discrepancy exists due to the approximation of TDS formulations. We also can see that there are big differences among $\sigma_{\phi\theta}$ with different κ_r. The cross-polarized RCS $\sigma_{\phi\theta}$ of the TDS with $\kappa_r = 0$ is very small and can be ignored when compared with those with $\kappa_r \neq 0$. With the increase of κ_r, the cross-polarized RCS is gradually increasing up covering the observed angles ranges from 120^{o} to 180^{o}. It confirms that the truth of one distinct manifestation of "chirality" is the existence of a cross-polarization component in the field scattered by a chiral object [12].

Finally, the TDS approximation is applied to calculate $\sigma_{\theta\theta}/\lambda_0^2$ and $\sigma_{\phi\theta}/\lambda_0^2$ of a thin chiral circular cylinder shell with radius 0.6 m, thickness 0.05 m, and height 0.2 m. The constitutive parameters are $\varepsilon_r = 2.6$, $\mu_r = 1$, and $\kappa_r = 0.0$, 0.2, 0.4, 0.6. The structure is illuminated by a plane wave incident from the direction where $(\theta, \varphi) = (0^{\circ}, 0^{\circ})$. Figure 4 (a) and (b) show the normalized co-polarized and cross-polarized bistatic RCS ($\sigma_{\theta\theta}/\lambda_0^2$ and $\sigma_{\phi\theta}/\lambda_0^2$) for scattering angle $\varphi = 0^{\circ}$, respectively. It is modeled by 480 triangles for the TDS SIE and 1038 tetrahedrons for VIE. The results when $\kappa_r = 0.2$ calculated by VIE (solid lines) are plotted for comparison. We can see from Fig. 4, the RCS results calculated by our code are in good agreements with those by VIE. It further confirms that the cross-polarization component in the field scattered by a chiral object is existing. It shows the superiority of the method used in the paper over VIE on the treatment of TDS.

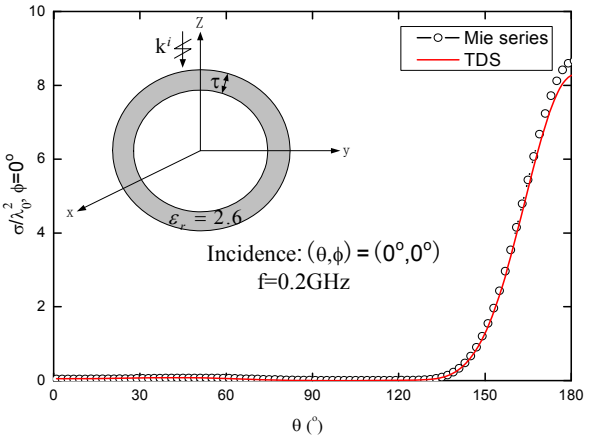

(a)

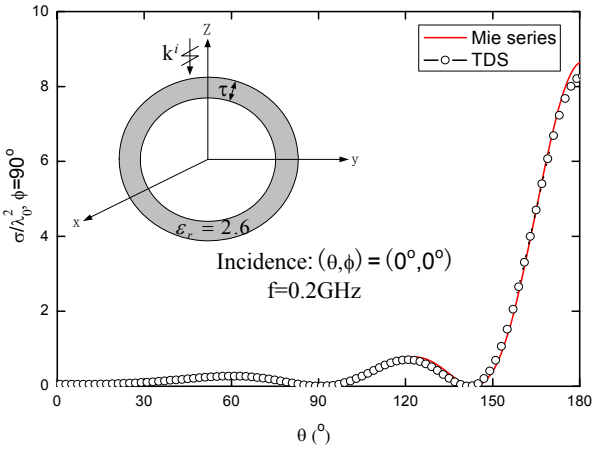

(b)

Fig. 2. Normalized total scattering cross section of a dielectric sphere shell in free space characterized by $\varepsilon_r = 2.6$, $\mu_r = 1$, $\kappa_r = 0$; (a) RCS at $\varphi = 0^{\circ}$ and (b) RCS at $\varphi = 90^{\circ}$.

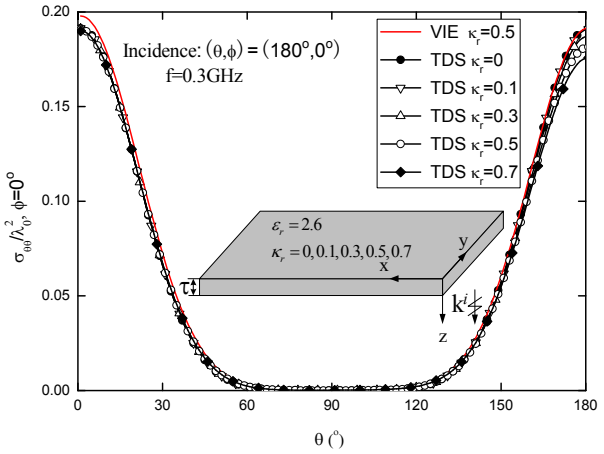

(a)

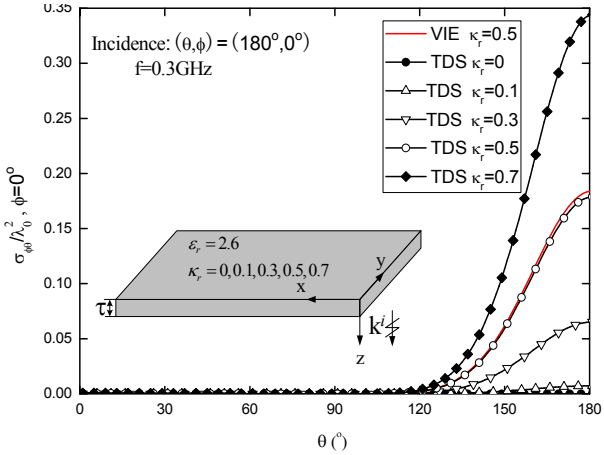

(b)

Fig. 3. Normalized scattering cross section of a thin chiral plate in free space characterized by $\varepsilon_r = 2.6$, $\mu_r = 1$, and $\kappa_r = 0, 0.1, 0.3, 0.5, 0.7$; (a) co-polarized and (b) cross-polarized components.

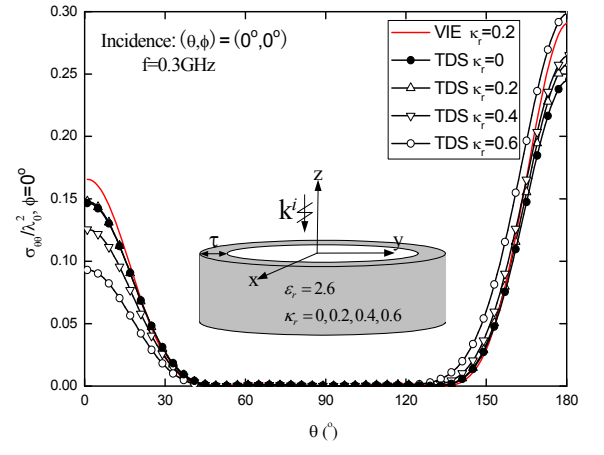

(a)

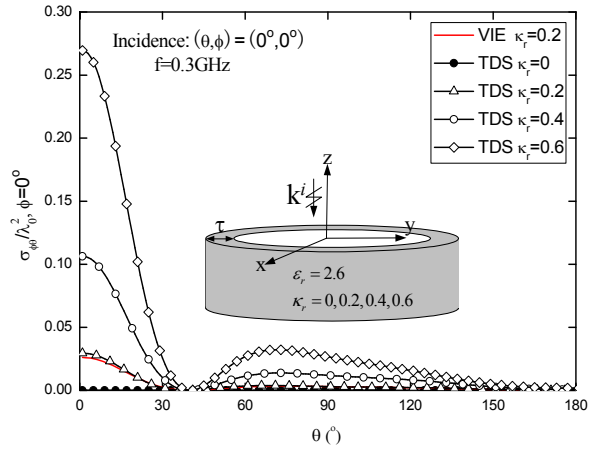

(b)

Fig. 4. Normalized scattering cross section of a chiral circular cylinder shell in free space characterized by $\varepsilon_r = 2.6$, $\mu_r = 1$, and $\kappa_r = 0, 0.2, 0.4, 0.6$; (a) co-polarized and (b) cross-polarized components.

IV. CONCLUSION

The TDS SIE method used in the paper leads to SIE instead of the traditional VIE. Consequently, the number of unknowns is reduced by only surface meshes being utilized to discretize the thin chiral dielectric sheet. Apparently, the approach in the paper needs fewer unknowns compared with VIE. In addition, it is easier for meshing. Modified RWG and pulse functions for basis and testing functions are employed to approximate the tangential and normal currents in the thin chiral dielectric layer. Finally, the TDS method are verified by Mie series and VIE by considering different shapes, and the simulation results show good agreements. Obviously, it is more advantageous to solve some thin sheet problems by TDS SIE than VIE. We further confirm that the truth of one distinct manifestation of "chirality" is the existence of a cross-polarization component in the field scattered by a chiral object in the paper.

The TDS approximation in the paper can deal with thin electric, chiral, and bi-isotropic media effectively. In spite of this, the method has its limitations because it is an approximate method. Scattering or radiation problems of a TDS coating metal are also of practical interest, the task is currently in progress and it will be reported later.

ACKNOWLEDGMENT

The work is supported by the National Nature Science Foundation of China under Grant No. 61071019, the Joint Funding projects of the Aerospace Science Foundation Office of China No. 2008ZA52006, the Innovation Program for Graduate Education of Jiangsu Province under Grant No. CXLX13_092.

APPENDIX

In this appendix, the parameters in equations (5), (6), (7), and (8) are given as,

$$\alpha_1 = \frac{\mu}{\varepsilon\mu - \zeta\xi} \tag{26}$$

$$\alpha_2 = \frac{-\xi}{\varepsilon\mu - \zeta\xi}\ , \tag{27}$$

$$\alpha_3 = \frac{-\zeta}{\varepsilon\mu - \zeta\xi}\ , \tag{28}$$

$$\alpha_4 = \frac{\varepsilon}{\varepsilon\mu - \zeta\xi}, \tag{29}$$

$$\beta_1 = \frac{\mu(\varepsilon - \varepsilon_0) - \zeta\xi}{\varepsilon\mu - \zeta\xi}\ , \tag{30}$$

$$\beta_2 = \frac{\xi\varepsilon_0}{\varepsilon\mu - \zeta\xi}, \tag{31}$$

$$\beta_3 = \frac{\zeta\mu_0}{\varepsilon\mu - \zeta\xi}\ , \tag{32}$$

$$\beta_4 = \frac{\varepsilon(\mu - \mu_0) - \zeta\xi}{\varepsilon\mu - \zeta\xi}\ . \tag{33}$$

Let us now consider the integrals in equations (17) and (18). According to [8], when τ is close to 0, the formulations (17) and (18) then can be approximated as,

$$\begin{aligned}\mathbf{E}_{die}^{scat}(\mathbf{r}) &= \omega^2\mu_0\tau\int_{S_{tds}} G(\beta_1\mathbf{D})dS' \\ &+\frac{\nabla}{\varepsilon_0}\left[\begin{array}{l}\tau\int_C G\Delta\beta_{1t}\mathbf{t}'\cdot\mathbf{D}_t dl' + \int_{S_n^+} G_T\Delta\beta_{1n}^+\mathbf{n}'\cdot\mathbf{D}_n^+ dS' \\ -\tau\int_{S_n^-} G\Delta\beta_{1n}^-\nabla_t'\cdot\mathbf{D}_t dS' - \int_{S_n^-} G\Delta\beta_{1n}^-\mathbf{n}'\cdot\mathbf{D}_n^+ dS'\end{array}\right] \\ &+\omega^2\mu_0\tau\int_{S_{tds}} G(\beta_2\mathbf{B})dS' \end{aligned} \tag{34}$$

$$\begin{aligned}&+\frac{\nabla}{\varepsilon_0}\left[\begin{array}{l}\tau\int_C G\Delta\beta_{2t}\mathbf{t}'\cdot\mathbf{B}_t dl' + \int_{S_n^+} G_T\Delta\beta_{2n}^+\mathbf{n}'\cdot\mathbf{B}_n^+ dS' \\ -\tau\int_{S_n^-} G\Delta\beta_{2n}^-\nabla_t'\cdot\mathbf{B}_t dS' - \int_{S_n^-} G\Delta\beta_{2n}^-\mathbf{n}'\cdot\mathbf{B}_n^+ dS'\end{array}\right] \\ &-i\omega\tau\beta_3\int_{S_{tds}}\nabla G\times\mathbf{D}dS' - i\omega\tau\beta_4\int_{S_{tds}}\nabla G\times\mathbf{B}dS'\end{aligned}$$

$$\begin{aligned}\mathbf{H}_{die}^{scat}(\mathbf{r}) &= \omega^2\varepsilon_0\tau\int_{S_{tds}} G(\beta_3\mathbf{D})dS' \\ &+\frac{\nabla}{\mu_0}\left[\begin{array}{l}\tau\int_C G\Delta\beta_{3t}\mathbf{t}'\cdot\mathbf{D}_t dl' + \int_{S_n^+} G_T\Delta\beta_{3n}^+\mathbf{n}'\cdot\mathbf{D}_n^+ dS' \\ -\tau\int_{S_n^-} G\Delta\beta_{3n}^-\nabla_t'\cdot\mathbf{D}_t dS' - \int_{S_n^-} G\Delta\beta_{3n}^-\mathbf{n}'\cdot\mathbf{D}_n^+ dS'\end{array}\right] \\ &+\omega^2\varepsilon_0\tau\int_{S_{tds}} G(\beta_4\mathbf{B})dS' \end{aligned} \tag{35}$$

$$\begin{aligned}&+\frac{\nabla}{\mu_0}\left[\begin{array}{l}\tau\int_C G\Delta\beta_{4t}\mathbf{t}'\cdot\mathbf{B}_t dl' + \int_{S_n^+} G_T\Delta\beta_{4n}^+\mathbf{n}'\cdot\mathbf{B}_n^+ dS' \\ -\tau\int_{S_n^-} G\Delta\beta_{4n}^-\nabla_t'\cdot\mathbf{B}_t dS' - \int_{S_n^-} G\Delta\beta_{4n}^-\mathbf{n}'\cdot\mathbf{B}_n^+ dS'\end{array}\right] \\ &-i\omega\tau\beta_1\int_{S_{tds}}\nabla G\times\mathbf{D}dS' - i\omega\tau\beta_2\int_{S_{tds}}\nabla G\times\mathbf{B}dS'\end{aligned}$$

here $G_T(\mathbf{r},\mathbf{r}') = G(\mathbf{r},\mathbf{r}'+\tau n')$, representing the contribution from the sources on the interface S_n^+. Note that $\mathbf{D}_n^-$ and $\mathbf{B}_n^-$ have been replaced by $\nabla_t\cdot\mathbf{D}_t$, $\mathbf{D}_n^+$ and $\nabla_t\cdot\mathbf{B}_t$, $\mathbf{B}_n^+$. And $\Delta\beta_{it} = \Delta\beta_{in}^+ = \Delta\beta_{in}^- = \beta_i\ (i = 1,2,3,4)$.

Then evaluations of the submatrices of the impedance matrix in equation (25) are,

$$Z_{TT,qd}^{DD} = \alpha_1 I_{tt1} - \omega^2\mu_0\tau\beta_1 I_{tt2} - \frac{\tau\beta_1}{\varepsilon_0} I_{tt3} + i\omega\tau\beta_3 I_{tt4} \tag{36}$$

$$Z_{TT,qd}^{DB} = \alpha_2 I_{tt1} - \omega^2\mu_0\tau\beta_2 I_{tt2} - \frac{\tau\beta_2}{\varepsilon_0} I_{tt3} + i\omega\tau\beta_4 I_{tt4}\ , \tag{37}$$

$$Z_{TT,qd}^{BD} = \alpha_3 I_{tt1} - \omega^2\mu_0\tau\beta_3 I_{tt2} - \frac{\tau\beta_3}{\varepsilon_0} I_{tt3} + i\omega\tau\beta_1 I_{tt4}\ , \tag{38}$$

$$Z_{TT,qd}^{BB} = \alpha_4 I_{tt1} - \omega^2\mu_0\tau\beta_4 I_{tt2} - \frac{\tau\beta_4}{\varepsilon_0} I_{tt3} + i\omega\tau\beta_2 I_{tt4}\ , \tag{39}$$

$$Z_{TN,qn}^{DD} = \alpha_1 I_{tn1} - \omega^2\mu_0\tau\beta_1 I_{tn2} - \frac{\beta_1}{\varepsilon_0} I_{tn3} + i\omega\tau\beta_3 I_{tn4}\ , \tag{40}$$

$$Z_{TN,qn}^{DB} = \alpha_2 I_{tn1} - \omega^2\mu_0\tau\beta_2 I_{tn2} - \frac{\beta_2}{\varepsilon_0} I_{tn3} + i\omega\tau\beta_4 I_{tn4}\ , \tag{41}$$

$$Z_{TN,qn}^{BD} = \alpha_3 I_{tn1} - \omega^2\mu_0\tau\beta_3 I_{tn2} - \frac{\beta_3}{\varepsilon_0} I_{tn3} + i\omega\tau\beta_1 I_{tn4}\ , \tag{42}$$

$$Z_{TN,qn}^{BB} = \alpha_4 I_{tn1} - \omega^2\mu_0\tau\beta_4 I_{tn2} - \frac{\beta_4}{\varepsilon_0} I_{tn3} + i\omega\tau\beta_2 I_{tn4}\ , \tag{43}$$

$$Z_{NT,md}^{DD} = \alpha_1 I_{nt1} - \omega^2\mu_0\tau\beta_1 I_{nt2} - \frac{\tau\beta_1}{\varepsilon_0} I_{nt3} + i\omega\tau\beta_3 I_{nt4}\ , \tag{44}$$

$$Z_{NT,md}^{DB} = \alpha_2 I_{nt1} - \omega^2\mu_0\tau\beta_2 I_{nt2} - \frac{\tau\beta_2}{\varepsilon_0} I_{nt3} + i\omega\tau\beta_4 I_{nt4}\ , \tag{45}$$

$$Z_{NT,md}^{BD} = \alpha_3 I_{nt1} - \omega^2\mu_0\tau\beta_3 I_{nt2} - \frac{\tau\beta_3}{\varepsilon_0} I_{nt3} + i\omega\tau\beta_1 I_{nt4}\ , \tag{46}$$

$$Z_{NT,md}^{BB} = \alpha_4 I_{nt1} - \omega^2 \mu_0 \tau \beta_4 I_{nt2} - \frac{\tau \beta_4}{\varepsilon_0} I_{nt3} + i\omega\tau\beta_2 I_{nt4}, \quad (47)$$

$$Z_{NN,mn}^{DD} = \alpha_1 I_{nn1} - \omega^2 \mu_0 \tau \beta_1 I_{nn2} - \frac{\beta_1}{\varepsilon_0} I_{nn3} + i\omega\tau\beta_3 I_{nn4}, \quad (48)$$

$$Z_{NN,mn}^{DB} = \alpha_2 I_{nn1} - \omega^2 \mu_0 \tau \beta_2 I_{nn2} - \frac{\beta_2}{\varepsilon_0} I_{nn3} + i\omega\tau\beta_4 I_{nn4}, \quad (49)$$

$$Z_{NN,mn}^{BD} = \alpha_3 I_{nn1} - \omega^2 \mu_0 \tau \beta_3 I_{nn2} - \frac{\beta_3}{\varepsilon_0} I_{nn3} + i\omega\tau\beta_1 I_{nn4}, \quad (50)$$

$$Z_{NN,mn}^{BB} = \alpha_4 I_{nn1} - \omega^2 \mu_0 \tau \beta_4 I_{nn2} - \frac{\beta_4}{\varepsilon_0} I_{nn3} + i\omega\tau\beta_2 I_{nn4}, \quad (51)$$

where

$$I_{tt1} = \int_{\partial T_q} \mathbf{f}_q \cdot \mathbf{f}_d ds, \quad (52)$$

$$I_{tt2} = \int_{\partial T_q} \int_{\partial T_d} G \mathbf{f}_q \cdot \mathbf{f}_d ds' ds, \quad (53)$$

$$I_{tt3} = \int_{\partial T_q} \int_C \mathbf{f}_q \cdot \nabla G\left(\mathbf{r}, \mathbf{r}' \in S_n^-\right) dl' ds - \int_{\partial T_q} \nabla_t' \cdot \mathbf{f}_d \int_{\partial T_d} \mathbf{f}_q \cdot \nabla G\left(\mathbf{r}, \mathbf{r}' \in S_n^-\right) ds' ds, \quad (54)$$

$$I_{tt4} = \int_{\partial T_q} \mathbf{f}_q \cdot \int_{\partial T_d} \nabla G \times \mathbf{f}_d ds' ds, \quad (55)$$

$$I_{tn1} = \int_{\partial T_q} \mathbf{f}_q \cdot \mathbf{n}_n ds, \quad (56)$$

$$I_{tn2} = \int_{\partial T_q} \mathbf{f}_q \cdot \int_{\partial T_d} G \mathbf{n}_n ds' ds, \quad (57)$$

$$I_{tn3} = \int_{\partial T_q} \mathbf{f}_q \cdot \nabla \int_{\partial T_d} G(\mathbf{r}, \mathbf{r}' \in S_n^+) \mathbf{n}' \cdot \mathbf{n}_n ds' ds - \int_{\partial T_q} \mathbf{f}_q \cdot \nabla \int_{\partial T_d} G(\mathbf{r}, \mathbf{r}' \in S_n^-) \mathbf{n}' \cdot \mathbf{n}_n ds' ds, \quad (58)$$

$$I_{tn4} = \int_{\partial T_q} \mathbf{f}_q \cdot \int_{\partial T_d} \nabla G \times \mathbf{n}_n ds' ds, \quad (59)$$

$$I_{nt1} = \int_{\partial T_m} \mathbf{n}_m \cdot \mathbf{f}_d ds, \quad (60)$$

$$I_{nt2} = \int_{\partial T_m} \mathbf{n}_m \cdot \int_{\partial T_d} G \mathbf{f}_d ds' ds, \quad (61)$$

$$I_{nt3} = \int_{\partial T_m} \mathbf{n}_m \cdot \nabla \int_C G(\mathbf{r}, \mathbf{r}' \in S_n^-) \mathbf{t}' \cdot \mathbf{f}_d dl' ds - \int_{\partial T_m} \mathbf{n}_m \cdot \nabla \int_{\partial T_d} G(\mathbf{r}, \mathbf{r}' \in S_n^-) \nabla_t' \cdot \mathbf{f}_d ds' ds, \quad (62)$$

$$I_{nt4} = \int_{\partial T_m} \mathbf{n}_m \cdot \int_{\partial T_d} \nabla G \times \mathbf{f}_d ds' ds, \quad (63)$$

$$I_{nn1} = \int_{\partial T_m} \mathbf{n}_m \cdot \mathbf{n}_n ds, \quad (64)$$

$$I_{nn2} = \int_{\partial T_m} \mathbf{n}_m \cdot \int_{\partial T_n} G \mathbf{n}_n ds' ds, \quad (65)$$

$$I_{nn3} = \int_{\partial T_m} \mathbf{n}_m \cdot \nabla \int_{\partial T_n} G(\mathbf{r}, \mathbf{r}' \in S_n^+) \mathbf{n}' \cdot \mathbf{n}_n ds' ds - \int_{\partial T_m} \mathbf{n}_m \cdot \nabla \int_{\partial T_n} G(\mathbf{r}, \mathbf{r}' \in S_n^-) \mathbf{n}' \cdot \mathbf{n}_n ds' ds, \quad (66)$$

$$I_{nn4} = \int_{\partial T_m} \mathbf{n}_m \cdot \int_{\partial T_n} \nabla G \times \mathbf{n}_n ds' ds. \quad (67)$$

Consider $\mathbf{t}' \cdot \mathbf{f}_d = 1$, $\mathbf{n}' \cdot \mathbf{n}_n = 1$ and $\int_s \mathbf{f} \cdot \mathbf{n} ds = 0$, then the above formulas become simple and easy to handle. It should note that $G(\mathbf{r}, \mathbf{r}' \in S_n^+) = G_T(\mathbf{r}, \mathbf{r}')$, representing the contribution from the sources on the interface S_n^+ . Consider,

$$\mathbf{n}(\mathbf{r}) \cdot \nabla G(\mathbf{r}, \mathbf{r}') = \frac{\partial G}{\partial n} \approx \frac{1}{\tau}\left[G\left(\mathbf{r} \in S_n^+, \mathbf{r}'\right) - G\left(\mathbf{r} \in S_n^-, \mathbf{r}'\right)\right] \quad (68)$$

then the integrations in equations (62) and (66) can be transformed to more simple forms, and then just integral of the Green's function needs to be treated, rather than that of the gradient of Green's function. After all these matrix elements have been evaluated, and then B_d , D_d , D_n , and B_n can be solved by direct or iterative matrix solvers.

REFERENCES

[1] V. Demir, A. Elsherbeni, and E. Arvas, "FDTD formulations for scattering from three dimensional chiral objects," *20th Annual Review of Progress in Applied Computational Electromagnetics (ACES)*, Syracuse, NY, April 2004.

[2] Y. Zhang, A. Bauer, and E. Li, "T-Matrix analysis of multiple scattering from parallel semi-circular channels filled with chiral media in a conducting plane," *Progress In Electromagnetics Research*, vol. 53, pp. 299-318, 2009.

[3] D. Worasawate, J. Mautz, and E. Arvas, "Electromagnetic scattering from an arbitrarily shaped three-dimensional homogeneous chiral body," *IEEE Trans. Antennas Propag.*, vol. 51, no. 5, pp. 1077-1084, May 2003.

[4] M. Hasanovic, C. Mei, J. Mautz, and E. Arvas, "Scattering from 3-D inhomogeneous chiral bodies of arbitrary shape by the method of moments," *IEEE Trans. Antennas Propag.*, vol. 55, no. 6, pp. 1817-1825, June 2007.

[5] T. Senior and J. Volakis, "Derivation and application of a class of generalized bound conditions," *IEEE Trans. Antennas Propag.* , vol. 37, pp. 1566-1572, 1989.

[6] R. Harrington and J. Mautz, "Impedance sheet approximation for thin dielectric shells," *IEEE Trans. Antennas Propag.*, vol. 23, no. 4, pp. 531-534, 1975.

[7] I. Chiang and W. Chew, "Thin dielectric sheet simulation by surface integral equation using modified RWG and pulse bases," *IEEE Trans. Antennas Propag.*, vol. 54, no. 7, pp. 1927-1934, July 2006.

[8] I. Chiang and W. Chew, "A coupled PEC-TDS surface integral equation approach for electromagnetic scattering and radiation from composite metallic and thin dielectric objects,"

IEEE Trans. Antennas Propag., vol. 54, no. 11, pp. 3511-3516, Nov. 2006.

[9] S. He, Z. Nie, S. Yan, and J. Hu, "Multi-layer TDS approximation used to numerical solution for dielectric objects," *Asia-Pacific Microwave Conference Proceedings*, APMC, 2008.

[10] S. He, Z. Nie, and J. Hu, "Numerical solution of scatter from thin dielectric-coated conductors based on TDS approximation and EM boundary conditions," *Progress In Electromagnetics Research*, vol. 93, pp. 339-354, 2009.

[11] S. Rao, D. Wilton, and A. Glisson, "Electromagnetic scattering by surfaces of arbitrary shape," *IEEE Trans. Ante nnas Propag.*, vol. 30, pp. 409-418, May 1982.

[12] A. Dmitrenko, A. Mukomolov, and V. Fisanov, "Scattering of electromagnetic waves on a magneto dielectric with chiral properties," *Russian Physics Journal*, vol. 39, no. 8, pp. 781-785, 1996.